

# Diffusion Tensor MRI Study of Myocardium Structural Remodeling after Infarction in Porcine Model

Yin Wu<sup>1,2</sup>, Hung-Fat Tse<sup>3</sup>, \*Ed. X. Wu<sup>1,2,4,5</sup>

Department of Electrical and Electronic Engineering<sup>1</sup>, Laboratory of Biomedical Imaging and Signal Processing-7T MRI Research Lab<sup>2</sup>, Department of Medicine<sup>3</sup>, Medical Engineering Program<sup>4</sup>, The Jockey Club MRI Centre<sup>5</sup>, The University of Hong Kong, Hong Kong SAR, China

\*Corresponding author: ewu@eee.hku.hk

**Abstract**— Investigation of infarct myocardium structure will lead to better understanding of functional adaptation and remodeling. Diffusion tensor magnetic resonance imaging (DTI) provides a means for rapid and nondestructive characterization of the three-dimensional fiber architecture of myocardium. DTI studies were performed on 10 excised, formalin-fixed hearts of both infarct (two months after left anterior descending coronary artery (LAD) occlusion surgery,  $n = 4$ ) and control ( $n = 6$ ) porcine. Each slice was divided into eight segments, and fractional anisotropy (FA) value and helix angle were measured in multiples short-axis slices, respectively. Infarct myocardium exhibited decreased FA value, flatter helix angle courses fluctuating around small helix angle with greater standard error of the mean (SEM) and smaller range of helix angle. The results provide structure information of infarct myocardium.

## I. INTRODUCTION

Study of the effects of a myocardial infarction (MI) on left ventricle (LV) function and structure has become a popular topic in recent years. Studies of these effects have shown changes that are not limited to the infarct-related area but also the adjacent and remote myocardium (1-6).

A wealth of study has discussed the influence of MI on LV function. Patten RD *et al* (1) found that hearts with MI exhibited lower systolic blood pressure, higher LV end-diastolic pressure, and increased LV mass-to-body weight ratio. Yang Z *et al* (2) studied changes of mass, end-systolic volume, end-diastolic volume, ejection fraction, cardiac output and percent wall thickening of LV 24 hours after MI. They found MI had little effect on LV end-diastolic volume but caused a 98% increase in end-systolic volume, which resulted in a significant reduction in ejection fraction. Wall thickening was depressed in both infarcted and remote myocardium. Bogaert J *et al* (3) focused on the morphology of MI heart using myocardial tagging. They found that circumferential and longitudinal radius of curvature was increased besides a significant increase in apical sphericity. A significant reduction in strain was observed in infarct, adjacent and remote myocardium.

For the remodeling of LV myocardium structure, Zimmerman SD *et al* (4) reported that noninfarcted tissue adjacent to the infarct remodeled by expansion along the direction of the fibers and in the cross fiber direction after myocardial infarction of three weeks. These data indicated that reorientation of fibers either via cell slippage or changes

in orientation of the laminar structure of the ventricular wall were quantitatively important aspects of the remodeling of the adjacent normally perfused myocardium. Fieno DS *et al* (5) measured the mass of both infarct and noninfarcted myocardium using gadolinium-enhanced MRI. They observed directionally opposite changes in resorption of infarcted tissue and compensatory hypertrophy of viable myocardium. Wall thinning occurred in all regions of the infarct expansion hearts compared with controls and was most pronounced in the infarct zone (6).

Diffusion tensor magnetic resonance imaging (DTI) has emerged as a powerful tool for rapid measurement of cardiac geometry and fiber structure with high spatial resolution at tissue and cellular level. DTI has been applied to investigate infarct myocardium structure recently. Hsu EW *et al* (7) studied delayed reduction of tissue water diffusion after myocardial ischemia. They found ADC of the nonperfused region showed a gradual but significant decreasing trend over time, whereas that of the normally perfused myocardium remained constant. The reduction of ADC may be linked to infarction which involves myocyte swelling. Chen J *et al* (8) reported that water diffusivity increased and diffusion anisotropy decreased in infarct rat myocardium four weeks after surgery. Besides, significant increase of angular deviation of the diffusion tensor was observed after myocardial infarction (8), but no change of fiber orientation was found at infarct myocardium (8, 9). However, the hearts examined in these studies only underwent early-stage infarction, when no apparent change occurred on wall thickness. In current study, infarct hearts were used to investigate remodeling myocardium structure after LAD occlusion surgery of two months when myocardium wall has become very thin.

## II. METHODS

### A. MR Imaging

Studies were performed on a Philips 3.0 Tesla Achieva scanner (Philips Medical System; Best; Netherlands) that has the maximum gradient amplitude of 80 mT/m and the gradient switch rate of 200 mT/m/s. An 8-channel head coil was used for imaging. The formalin-fixed porcine heart samples were suspended in a cylinder filled with formalin to avoid tissue-air susceptibility artifacts. Scout images were

first acquired on right anterior oblique and nearly four-chamber planes, which were perpendicular to each other. LV long axis was determined as the intersecting line of the two planes that divided the LV equally into four quadrants from base to apex. LV short-axis planes were prescribed as perpendicular to the LV long axis and covered the entire heart. DTI was performed using single-shot spin echo, echo planar imaging (SE-EPI). Sensitivity-encoding (SENSE) was applied to shorten image acquisition time and to alleviate image distortion caused by susceptibility artifact from single-shot EPI sequences. SENSE factor was chosen to be 2.4 in this study to trade off between image distortion due to high EPI factor and SENSE artifact caused by high sense factor. Imaging parameters were the following: TE = 45 ms; TR = 4.0 s; FOV = 140×140 mm<sup>2</sup>; slice thickness = 1.13 mm; slice gap = 0 mm; diffusion sensitivity of b = 800 s/mm<sup>2</sup>; gradient direction = 15; and number of averages = 40. In this study, images were acquired with a 128×128 data matrix. These parameters yielded an isotropic resolution of 1.13×1.13×1.13 mm<sup>3</sup>. Depending on the heart sample size, the slice number was typically around 45. Total image acquisition time was about 1 hr per sample.

### B. Data Processing

Three-dimensional reconstruction of myocardial fiber tracks and FA value were obtained by using the PRIDE software package (Philips Medical Systems; Best; Netherlands). Papillary muscles and right ventricles were removed in the images and excluded from the analysis. For each of the short-axis slices, the fiber was tracked pixel by pixel within the slice. A MATLAB (The MathWorks, Natick, MA) program was developed to compute the fiber orientation from the data generated from PRIDE software. The myocardial fiber orientation was calculated by first

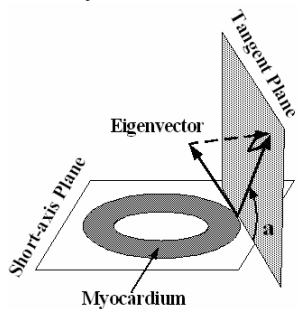


Fig.1 Fiber helix angle  $\alpha$ , which is defined as the angle between the projection of the primary eigenvector onto the tangent plane and the short-axis imaging plane

transforming the primary eigenvector from the Cartesian

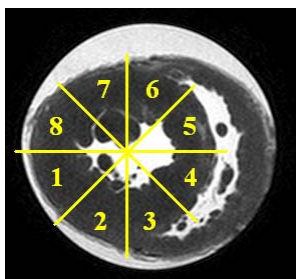


Fig.2 Slice was divided into eight segments going counterclockwise as viewed from the base: posterolateral wall, left posterior wall, right posterior wall, posterior septum, anterior septum, right anterior wall, left anterior wall and anterolateral wall, corresponding to ROI 1 to ROI 8.

coordinates to the local cylindrical myocardial coordinates

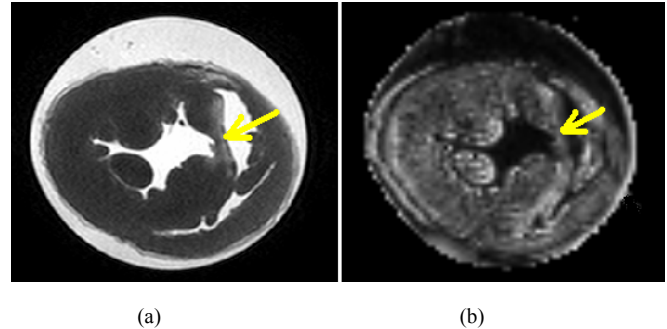


Fig.3 T2-weighted image (a) and FA magnitude map (b) of an infarct slice. Infarct region indicated by yellow arrows is very thin.

that are centered at the LV center. The epicardial tangent planes are defined as the planes tangent to the epicardial circle and parallel to the LV long axis as proposed by Scollan *et al* (10) (Fig.1). After determining the local myocardial coordinate system for each short-axis slice, fiber helix angle was calculated for each fiber tracked within the slice. Fiber helix angle is defined as the angle between the projection of the primary eigenvector onto the tangent plane and the short-axis imaging plane (Fig. 1). Each slice was further divided into eight segments going counterclockwise as viewed from the base: posterolateral wall, left posterior wall, right posterior wall, posterior septum, anterior septum, right anterior wall, left anterior wall and anterolateral wall, corresponding to ROI 1 to ROI 8 (Fig.2). Average FA value and transmural variations of the fiber helix angle were measured in each segment. Center of infarct myocardium was aligned to the same location within the infarct group. Unless otherwise noted, all data are presented as means  $\pm$  SEM.

## III. RESULTS

### A. Fractional Anisotropy

T2-weighted image (a) and FA magnitude map (b) of an infarct slice were shown in Fig.3. Infarct region indicated by red arrows is very thin.

FA value was normalized for each heart sample. Fig.4 illustrates FA map of controls ( $n = 6$ ) (Fig.4 (a)) and one infarct heart (Fig.4 (b)). FA value is much more homogeneous in controls compared with that of infarct one, in which FA value decreases gradually from normal to the

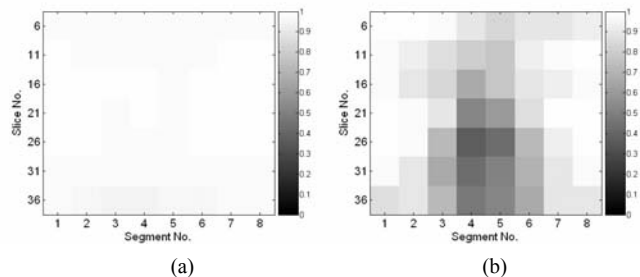


Fig.4 FA map of controls ( $n = 6$ ) (a) and one infarct heart (b). FA value is much more homogeneous in controls compared with that of infarct one, in which FA value decreases gradually from normal to the center of infarct segment (segment 4 of slice 26).

center of infarct segment (segment 4 of slice 26). Adjacent area was influenced as well but less pronouncedly. Similar FA maps can be observed on the other three infarct hearts. Maximum FA value decrease of control and infarct hearts were illustrated in Table 1, which shows that FA value decreases significantly in infarct group. These results are due to the fact that myocardium with infarction was swelling and reducing the isotropic characteristics of myocardial fiber (7).

TABLE 1  
MAXIMUM FA VALUE DECREASE

	Controls (n = 6)	Infarct heart #1	Infarct heart #2	Infarct heart #3	Infarct heart #4
Maximum FA value	3.1	35.2	41.6	44.8	55.4
decrease (%)					

### B. Helix Angle of Myocardial Fiber

Two representative slices, with and without infarction, were selected from infarct group to investigate the helix angle variations with transmural depth. Two slices at the same anatomic location were chosen from controls as reference. Results were shown in Fig.5. The helix angle changes roughly from 60° at the endocardium to -40° at the epicardium in controls. No significant difference was observed in the trend of helix angle courses among different segments or slices. In all the segments of slice without infarction and the remote and adjacent segments of slice with infarction (Fig.5(b), ROI 1-2 and 6-8) of infarct group, courses of helix angle deviate from that of controls, which may due to the specific choice of LV long axis and LV center (8). However, transmural courses of helix angle are significantly different from that of controls in infarct segment (Fig.5(b), ROI 3-5) with larger angular SEM, which was about 4.29±0.23° in the controls and increased to 10.25±1.40° in the infarct group. Helix angle courses tended to be flatter and fluctuant around small helix angle. It is likely that fibers become more circumferentially orientated in infarction region after remodeling. Range of helix angle was compared between two groups and results show that the range is smaller in infarct segments (39.7±29.9°, 54.4±25.2°, 52.9±32.1° in ROI 3-5, respectively) than that of controls (87.4±10.8°, 102.1±12.9°, 101.9±6.8° in ROI 3-5, respectively) (Fig.6(b)). Therefore, greater regional variations in fiber helix angle occur at infarct myocardium.

## IV. DISCUSSION AND CONCLUSION

In summary, FA value and fiber helix angle courses were investigated in control and infarct porcine hearts using diffusion tensor MRI. FA value decreases gradually from normal to infarct region in infarct hearts. Helix angle courses tend to be flatter and fluctuant around small helix angle with larger angular SEM and smaller range of helix angle in

infarct regions. These results provide myocardium structure information after late-stage infarction.

## ACKNOWLEDGMENT

The authors acknowledge the Laboratory of Animal Unit of the Department of Medicine, The University of Hong Kong, for preparing porcine heart samples. This work was in part supported by the Hong Kong Jockey Club Charities Trust, CRCG grants and HKU Seed Funding.

## REFERENCES

- [1] Patten RD, Aronovitz MJ, Deras-mejia L, Pandian NG, Hanak GG, Smith JJ, Mendelsohn ME, Konstam MA. Ventricular remodeling in a mouse model of myocardial infarction. *Am. J. Physiol* 1998; 43:H1812-H1820
- [2] Yang Z, Berr SS, Gilson WD, Toufektsian MC, French BA. Simultaneous evaluation of infarct size and cardiac function in intact mice by contrast-enhanced cardiac magnetic resonance imaging reveals contractile dysfunction in noninfarcted regions early after myocardial infarction. *Circulation* 2004;109:1161-1167
- [3] Bogaert J, Bosmans H, Maes A, Suetens P, Marchal G, Rademakers FE. Remote myocardial dysfunction after acute anterior myocardial infarction: impact of left ventricular shape on regional function. *Journal of the American College of Cardiology* 2000;35:1525-1534
- [4] Zimmerman SD, Criscione J, Covell JW. Remodeling in myocardium adjacent to an infarction in the pig left ventricle. *Am J Physiol Heart Circ Physiol* 2004;287:H2697-H2704
- [5] Fieno DS, Hillenbrand HB, Rehwald WG, Harris KR, Decker RS, Parker MA, Klocke FJ, Kim RJ, Judd RM. Infarct resorption, compensatory hypertrophy, and differing patterns of ventricular remodeling following myocardial infarctions of varying size. *Journal of American College of Cardiology* 2004;43:2124-2131
- [6] Weisman HF, Bush DE, Mannisi JA, Weisfeldt ML, Healy B. Cellular mechanisms of myocardial infarct expansion. *Circulation* 1988;78:186-201
- [7] Hsu EW, Xue R, Holmes A, Forder JR. Delayed reduction of tissue water diffusion after myocardial ischemia. *Am J Physiol* 1998;44:H697-702
- [8] Chen J, Song SK, Liu W, McLean M, Allen JS, Tan J, Wickline SA, Yu X. Remodeling of cardiac fiber structure after infarction in rats quantified with diffusion tensor MRI. *Am J Physiol Heart Circ Physiol* 2003;285:H946-954
- [9] Walker JC, Guccione JM, Jiang Y, Zhang P, Wallave AW, Hsu EW, Ratcliffe MB. Helical myofiber orientation after myocardial infarction and left ventricular surgical restoration in sheep. *The Journal of Thoracic and Cardiovascular Surgery* 2005;382-390.
- [10] Scollan DF, Holmes A, Winslow R, Forder J. Histological validation of myocardial microstructure obtained from diffusion tensor magnetic resonance imaging. *Am J Physiol Heart Circ Physiol* 1998;275:H2308-H2318.

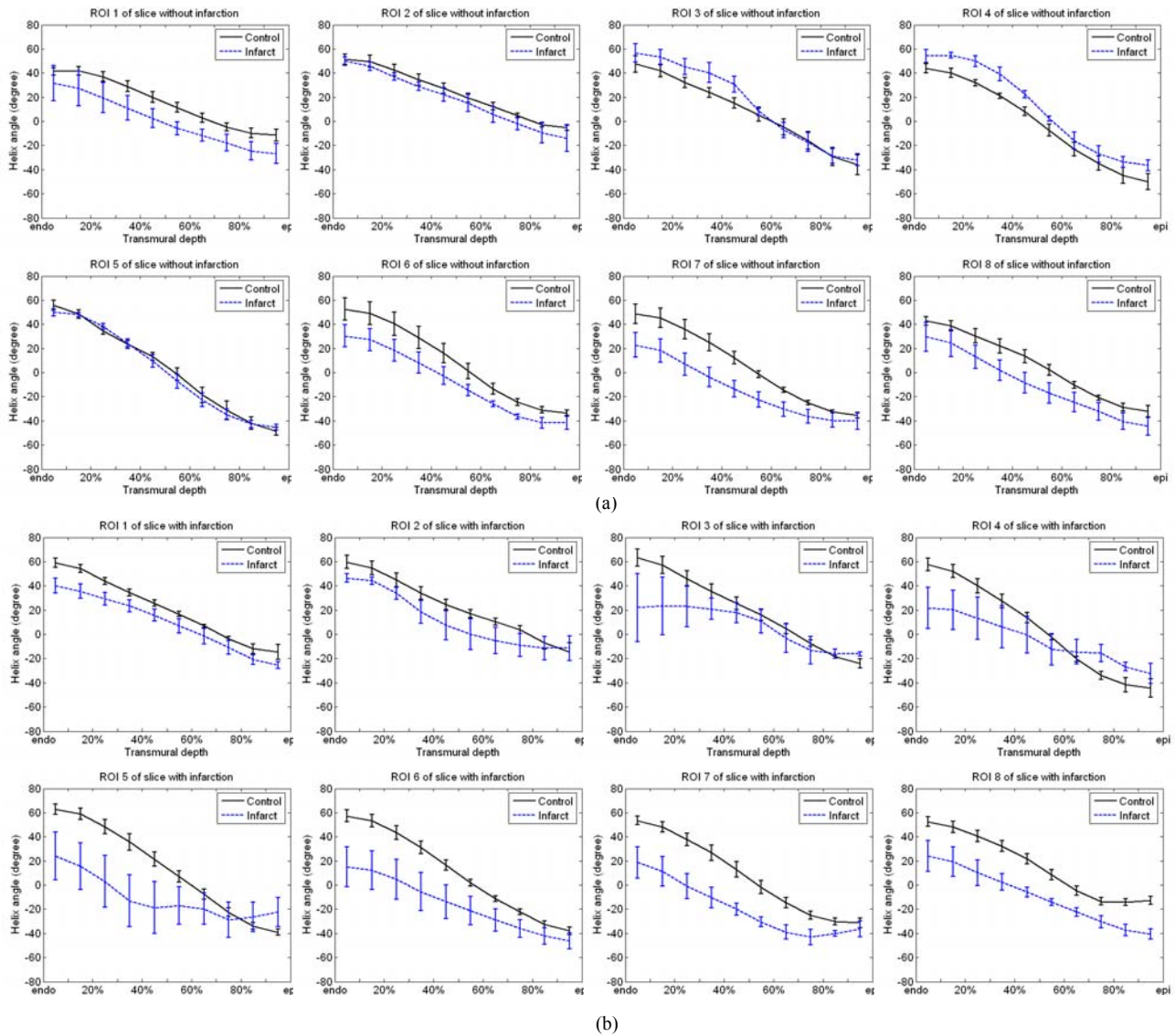


Fig.5 Helix angle courses of two representative slices, without infarction (a) and with infarction (b) of control and infarct group. The helix angle changes roughly from  $60^\circ$  at the endocardium to  $-40^\circ$  at the epicardium in control. No significant difference was observed in the trend of helix angle courses among different segments or slices. In all the segments of slice without infarction and the remote and adjacent segments of slice with infarction ((b), ROI 1-2 and 6-8) of infarct group, courses of helix angle deviate from that of control, which may due to the specific choice of LV long axis and LV center. However, transmural courses of helix angle are significantly different from that of control in infarct segment ((b) ROI 3-5) with larger angular SEM, which was about  $4.29 \pm 0.23^\circ$  in the control and increased to  $10.25 \pm 1.40^\circ$  in the infarct group. Helix angle courses tended to be flatter and fluctuant around small helix angle.

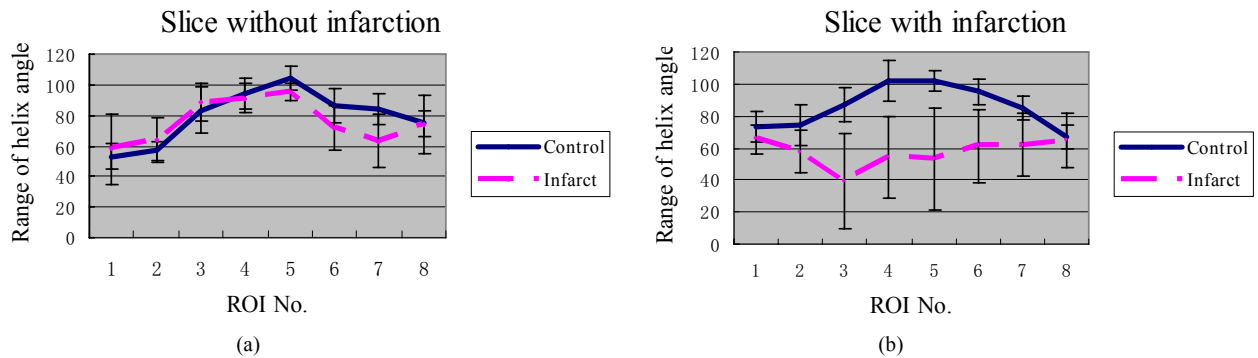


Fig.6 Range of helix angle of two representative slices, without infarction (a) and with infarction (b) of control and infarct group. The range is smaller in infarct segments ( $39.7 \pm 29.9^\circ$ ,  $54.4 \pm 25.2^\circ$ ,  $52.9 \pm 32.1^\circ$  in ROI 3-5, respectively) than that of controls ( $87.4 \pm 10.8^\circ$ ,  $102.1 \pm 12.9^\circ$ ,  $101.9 \pm 6.8^\circ$  in ROI 3-5, respectively) (b).